

Volume Density of Power of Multivector Electric Machine

Aldan A. Sapargaliyev, Yerbol A. Sapargaliyev

Abstract—Since the invention, the electric machine (EM) can be defined as oEM – one-vector electric machine, as it works due to one-vector inductive coupling with use of one-vector electromagnet. The disadvantages of oEM are large size and limited efficiency at low and medium power applications. This paper describes multivector electric machine (mEM) based on multi-vector inductive coupling, which is characterized by the increased surface area of the inductive coupling per EM volume, with a reduced share of inefficient and energy-consuming part of the winding, in comparison with oEM's. Particularly, it is considered, calculated and compared the performance of three different electrical motors and their power at the same volumes and rotor frequencies. It is also presented the result of calculation of correlation between power density and volume for oEM and mEM. The method of multi-vector inductive coupling enables mEM to possess 1.5-4.0 greater density of power per volume and significantly higher efficiency, in comparison with today's oEM, especially in low and medium power applications. mEM has distinct advantages, when used in transport vehicles such as electric cars and aircrafts.

Keywords—Electric machine, electric motor, electromagnet, efficiency of electric motor.

I. INTRODUCTION

ANY EM includes the system of induction-interacting blocks (SIB), consisting of at least two subsystems of induction-interacting blocks (SSIB) that are movable relative to each other, wherein at least one induction-interacting block is the electromagnetic block.

Currently, in the world practice, EM utilises one type of winding of an electromagnet – *one-vector winding* (oW). Figs. 1-3 show conventional types of oW in coordinate system xyz (Fig. 4): *collected* oW.0, *semi-collected* oW.1 and *dispersed* oW.2, with incoming $w1$ and outgoing $w2$ winding parts. In this regard, on Figs. 1-3, the useful parts of windings are separated from the rest of the windings by planes P_{pj} , where $j=1, 2, 3$. In all three types of oW on Figs. 1-3, only the specified straight sections of the winding contribute to the required electromagnetic cohesion:

- four parts in collected winding oW.0: $p1$, $p2$, $p\tau1$ and $p\tau2$;
- three parts in the semi-collected winding oW.1: $p1$, $p2$ and $p\tau1$; part $p01$ can be utilized in other windings;
- in the dispersed winding oW.2, two parts of the winding: $p1$ and $p2$; parts $p01$ and $p02$ can be utilized in other windings.

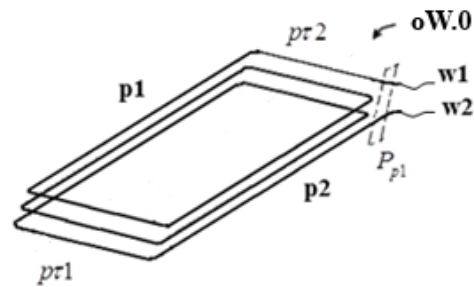


Fig. 1 Collected winding oW.0

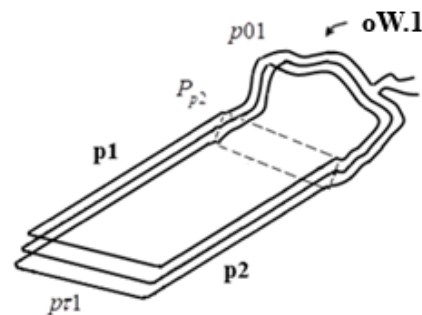


Fig. 2 Semi-collected winding oW.1

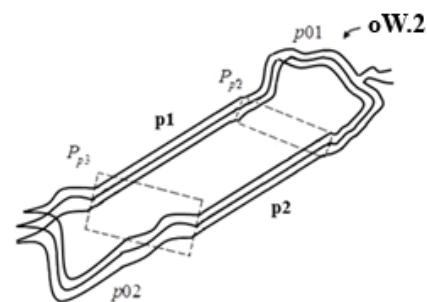


Fig. 3 Dispersed winding oW.2

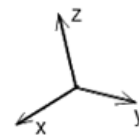


Fig. 4 System of coordinates for spatial position on Figs. 1-3

Two sides of the surface between two lateral winding parts $p1$ and $p2$ form two sides of oW. Two sides of oW from the side of its transverse parts $p\tau1$ and $p\tau2$ form two end sides of the oW.

In the future, with respect to any windings, we will adhere to the coordinate system introduced on Fig. 4 with respect to the spatial orientation of the geometry of an electromagnet windings: $xz(A)$ -plane, which is a vertical plane, will be called $xz(A)$ -plane or \hat{h} -plane; $zy(A)$ -plane is the upper plane of an electromagnet, will be called $zy(A)$ -plane or ω -plane; the xy -plane is a lateral plane, will be called the $xy(A)$ -plane or $\hat{\lambda}$ -plane. It is assumed that the main plane where the induction cohesion takes place is the $\hat{\lambda}$ -plane. The distance between two sides $p1$ and $p2$ of winding parts is the width of the winding, the distance between the two transverse sides $pr1$ and $pr2$ of winding parts is the winding height.

There are three types of SIB for three types of EM that are based on oW . They are shown on Figs. 5-7: one-side $oSB.1$ [1]-[3]; vertical-scan two-sided $oSB.2$, which is called as *dual-rotor* [4], [5]; horizontal-scan integrated $oSB\Sigma$ (a system containing a lot of $oSB.2$ located along their common axial direction), which is called as *pancake-type motor* [6-8].

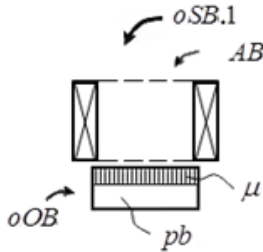


Fig. 5 One-sided $oSB.1$

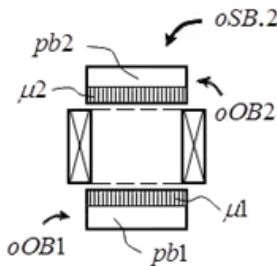


Fig. 6 Vertical-scan two-sided $oSB.2$

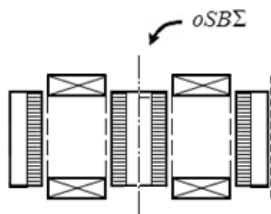


Fig. 7 Horizontal-scan integrated $oSB\Sigma$

On Figs. 5-7 the following designations are introduced: side oOB (oOB - one-vector off-source block), first side $oOB1$ and second side $oOB2$; an induction-inhomogeneous environment μ , a first induction-inhomogeneous environment $\mu1$, a second induction-inhomogeneous environment $\mu2$, respectively, of the side oOB , of the first side $oOB1$ and of the

second side $oOB2$; bridge/bus pb , first bridge/bus $pb1$, second bridge/bus $pb2$ of magnetic field, respectively, of the side oOB , of the first side $oOB1$ and of the second side $oOB2$.

II. HARMONIC MULTI-VECTOR ELECTRIC MACHINE

In order to create a small-sized EM with a high output power, it is possible to use multi-vector electromagnets, based on multi-vector electromagnet windings [9]. Multi-vector winding provides the possibility of: large density of induction per volume, compared to that one of one-vector winding; reduction of the volume of the winding wire. From the manifold of multi-vector windings presented in [9], we consider only some of them shown on Figs. 8-11, two-side Λ -shaped (or U-shaped) windings.

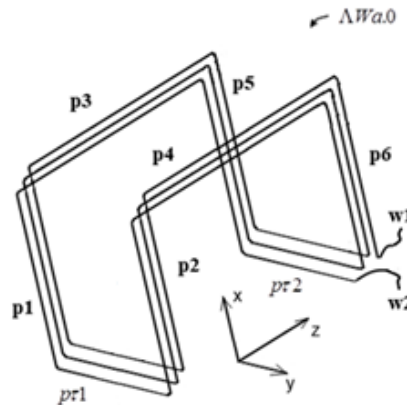


Fig. 8 A single collected winding $\Lambda Wa.0$

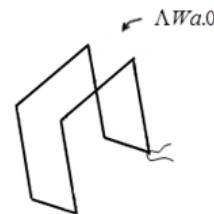


Fig. 9 $\Lambda Wa.0$ is shown with coils in a merged form

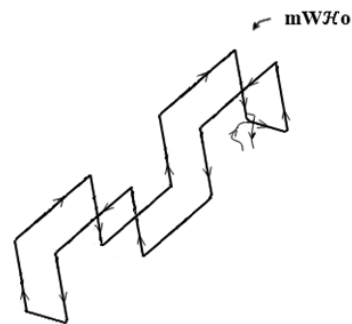


Fig. 10 Multi-vector harmonic winding $mW\mathcal{H}o$ in a merged form

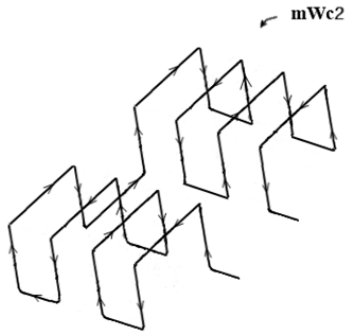


Fig. 11 Multi-vector harmonic winding $mWc2$ in a merged form

Fig. 8 shows a three-dimensional image of a multi-vector parallel two-sided single collected winding $\Lambda Wa.0$ with a straight upper side. ΛWa , as well as its oW analogue, could be performed with the incoming and outgoing parts of the winding – a single semi-collected and single dispersed. On Fig. 9 coils of a multi-vector two-side single collected winding are presented, in a merged form for the simplicity. On Figs. 10 and 11, two kinds of harmonic-multi-vector windings $mW\mathcal{H}o$ and $mWc2$ are presented. To compare the performance of one-vector and multi-vector EM on Figs. 12-14, three EMs are shown in coordinate yz -plane, respectively:

- multi-vector harmonic electric machine $mEM\mathcal{H}$ with multi-vector harmonic system block, consisting of multi-vector harmonic electromagnetic block $mAB\mathcal{H}$ and multi-vector integrated off-source block $mOB\mathcal{H}$;
- one-vector single $oEMo$ electric machine with one-vector single system block consisting of one-vector single electromagnetic block $oABo$ and one-vector single off-source block $oOBo$;
- one-vector in-line electric machine $oEM\Sigma$ with one-vector in-line system block, consisting of one-vector in-line electromagnetic block $oAB\Sigma$ and one-vector in-line single off-source block $oOB\Sigma$.

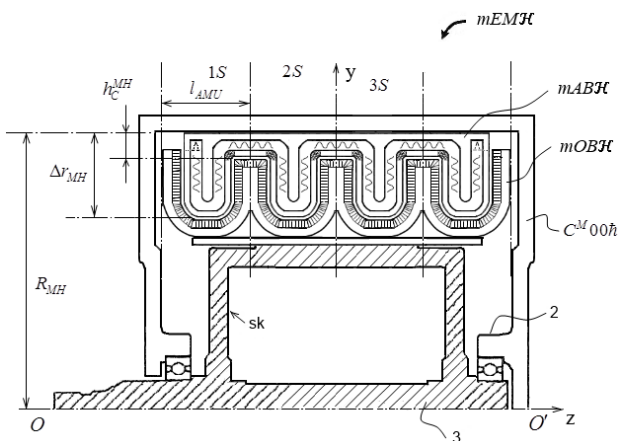


Fig. 12 Multi-vector Electric Machine $mEM\mathcal{H}$

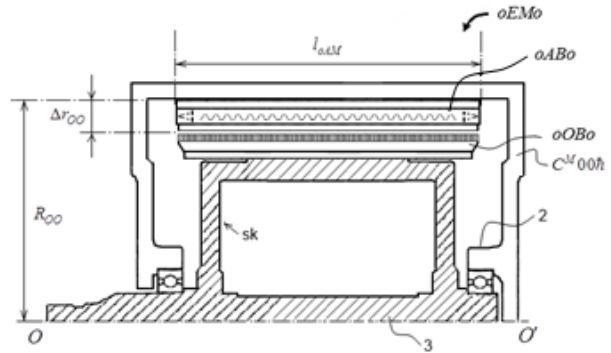


Fig. 13 One-vector Electric Machine $oEMo$

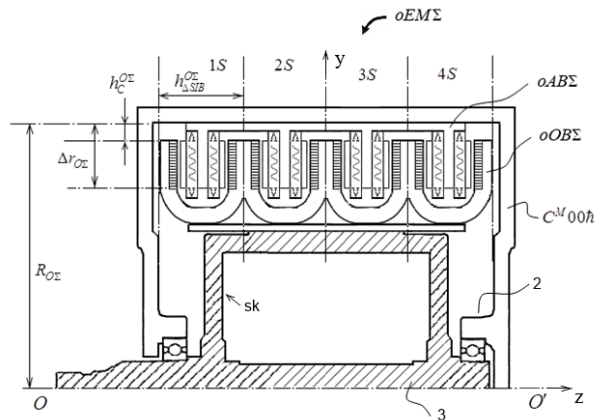


Fig. 14 One-vector Electric Machine $oEM\Sigma$

On Figs. 12-14, the following notations are introduced: sk – k -th prop to a off-source block; 3 – bushing; 2 – shaft; C^M00h – case.

The value of mechanical power of a shaft of a rotating electric motor [10], [11] is defined by:

$$P = M\omega = Fr\omega \tag{1}$$

where P – power (W), ω – Angular frequency (rad/sec), M – rotational moment (Nm), F – force (N), r – Radius vector (m).

Assuming, for all three EMs:

$$\begin{aligned} \omega_{MH} &= \omega_{OO} = \omega_{O\Sigma} = \omega_{EM}, \\ V_{MH} &= V_{OO} = V_{O\Sigma} = V_{EM}, \\ R_{MH} &= R_{OO} = R_{O\Sigma} = R_{EM}, \end{aligned}$$

(i.e., with the same rotation frequency of the rotors ω_{EM} , volumes V_{EM} , external SIB radii R_{EM} for all three EMs), the mathematical model of the ratio of the volume density of power by volume of EM has the following view

$$\frac{N_{MH/V}}{N_{OS/V}} = \frac{[2R_{EM} - (\Delta r_{MH} + h_C^{MH})][\Delta r_{MH} + 3h_C^{MH}(\frac{k-2}{2k})]}{(2R_{EM} - \Delta r_{OS})(\Delta r_{MH} - h_C^{OS})} \quad (2)$$

$$\frac{N_{MH/V}}{N_{OO/V}} = \frac{[2R_{EM} - (\Delta r_{MH} + h_C^{MH})][\Delta r_{MH} + h_C^{MH}(3 - \frac{2}{2k})]}{5h_C^{MH}(R_{EM} - h_C^{OO})} \quad (3)$$

where k – numerical coefficient $k = 2,6,8,10,12,14,\dots$, $N_{MH/V}$, $N_{OS/V}$ and $N_{OO/V}$ are values of power density by volume of, respectively: multi-vector harmonic $mEM\mathcal{H}$; one-vector in-line $oEM\Sigma$ one-vector single $oEMo$. In this case, certain EM constructions are considered under assumption that all three EMs have the same:

- thickness of windings h_C^{MH} equal to $h_C^{MH} = h_C^{OS} = h_C^{OO} = h_C^{MH}$;
- width of the off-source block Δh_{SIB}^{OS} and width of the SIB period Δh_{SIB}^{MH} that are equal to $\Delta h_{SIB}^{MH} = \Delta h_{SIB}^{OS} = 5h_C^{MH}$;
- height of the electromagnetic block Δr_{MH} , the value of which is limited within $5h_C^{MH} \leq \Delta r_{MH} \leq 15h_C^{MH}$.

III. THE COMPARISON

The results of calculations $\frac{N_{EM/V}}{N_{OS/V}}$ and $\frac{N_{EM/V}}{N_{OO/V}}$ for variations in geometry of EMs are given in Tables I and II. It can be seen from the tables that the mean values of the ratio of power density by volume of EM are limited within $1,1 \leq \frac{N_{EM/V}}{N_{OS/V}}$

$\leq 1,5$ and $1,4 \leq \frac{N_{EM/V}}{N_{OO/V}} \leq 4,4$. They show that mEMs have a

much higher power density by volume in comparison with the similar indicators of oEMs. Moreover, in $mEM\mathcal{H}$, the ratio of the lengths of the longitudinal working part to the end non-working part of the windings is greater than that in $oEM\Sigma$, and therefore the efficiency of $mEM\mathcal{H}$ is greater than that of $oEM\Sigma$.

TABLE I
RESULTS FOR $\frac{N_{EM/V}}{N_{OS/V}}$

| | K=2 | | K=6 | | K→∞ | |
|----------------------------------------------|--------------|--------------|--------------|--------------|-------------|--------------|
| Δr_{MH} | $5h_C^{MH}$ | $15h_C^{MH}$ | $5h_C^{MH}$ | $15h_C^{MH}$ | $5h_C^{MH}$ | $15h_C^{MH}$ |
| $\frac{\Delta r_{MH}}{R_{EM}} = \frac{1}{3}$ | $1,046 \leq$ | $\leq 1,27$ | $1,113 \leq$ | $\leq 1,593$ | $1,180 <$ | $< 1,756$ |
| $\frac{\Delta r_{MH}}{R_{EM}} \rightarrow 0$ | $1,09 \leq$ | $\leq 1,33$ | $1,18 \leq$ | $\leq 1,66$ | $1,23 <$ | $< 1,83$ |

TABLE II
RESULTS FOR $\frac{N_{EM/V}}{N_{OO/V}}$

| | K=2 | | K=6 | | K→∞ | |
|----------------------------------------------|-------------|--------------|-------------|--------------|-------------|--------------|
| Δr_{MH} | $5h_C^{MH}$ | $15h_C^{MH}$ | $5h_C^{MH}$ | $15h_C^{MH}$ | $5h_C^{MH}$ | $15h_C^{MH}$ |
| $\frac{\Delta r_{MH}}{R_{EM}} = \frac{1}{3}$ | $1,37 \leq$ | $\leq 4,11$ | $1,71 \leq$ | $\leq 4,45$ | $1,88 <$ | $< 4,62$ |
| $\frac{\Delta r_{MH}}{R_{EM}} \rightarrow 0$ | $1,6 \leq$ | $\leq 4,8$ | $2 \leq$ | $\leq 5,2$ | $2,2 <$ | $< 5,4$ |

IV. CONCLUSION

mEM, unlike oEM, has a large constructive variety and mEM \mathcal{H} is one of its subspecies. At present, the first laboratory prototype of mEM is built and is going to be presented at Expo-2017 in Astana. It is foreseen with great probability that industrial prototypes of mEM will appear by the end of 2018, and in a short time mEMs are able not just oust the widely used oEM from the world market, but also suggest new applications.

REFERENCES

- [1] J. Matt and J. Legranger, "Synchronous rotating electrical machine with permanent magnets and flux concentration", U.S. Patent 8 508 094, August 13, 2013.
- [2] N. Hino, Y. Matsunobu, S. Sugimoto and A. Kamiya, "Rotary electric machine with air gaps configured to cancel torque pulsations", U.S. Patent 8 368 273, February 5, 2013.
- [3] M. Kuroda, "Small DC motor", U.S. Patent 8 013 489, September 6, 2011.
- [4] B. S. Shaw, "Brushless disk DC motor", U.S. Patent US7898134, March 1, 2011.
- [5] J. Ritchey, "Poly-phasic multi-coil generator", U.S. Patent 20 080 088 200, April 17, 2008.
- [6] D. L. Guo, K. Lu, M. H. Lin and T. C. Song, "Brushless motor having coreless assembly", U.S. Patent 20 060 244 320, November 2, 2006.
- [7] Y. Asano, "Axial gap rotary electric machine and rotary driving device", U.S. Patent 8 242 661, August 14, 2012.
- [8] T. Woolmer, "Electric machine - over-moulding construction", U.S. Patent 20 130 147 291, June 13, 2013.
- [9] A. A. Sapargaliyev, "Multiple-vector inductive coupling and electric machine", WO2015137790, November 12, 2015.
- [10] I. V. Savelyev, "Course of General Physics (mechanics, oscillations and waves, molecular physics)," Moscow: Nauka, vol.1, 1970.
- [11] J. L. Kirtley Jr., "Class Notes 1: Electromagnetic Forces. 6.6585 - Electric Machines," MIT Dept of Electrical Engineering. Retrieved 15 March 2013.